# Configuration Studies for an ST-Based Fusion Nuclear Science Facility

J. Menard[1], M. Boyer[1], T. Brown[1], J. Canik[2], B. Covele[3], C. D'Angelo[4], A. Davis[4], L. El-Guebaly[4], S. Gerhardt[1], S. Kaye[1], C. Kessel[1], M. Kotschenreuther[3], S. Mahajan[3], R. Maingi[1], E. Marriott[4], L. Mynsberge[4], C. Neumeyer[1], M. Ono[1], R. Raman[5], S. Sabbagh[6], V. Soukhanovskii[7], P. Valanju[3], R. Woolley[1], and A. Zolfaghari[1]

[1]Princeton Plasma Physics Laboratory, Princeton, NJ 08543
[2]Oak Ridge National Laboratory, Oak Ridge, TN, USA
[3]University of Texas, Austin, TX, USA
[4]University of Wisconsin, Madison, WI, USA
[5]University of Washington, Seattle, WA, USA
[6]Columbia University, New York, NY, USA
[7]Lawrence Livermore National Laboratory, Livermore, CA, USA

*E-mail contact of main author: jmenard@pppl.gov*

**Abstract**. A Fusion Nuclear Science Facility (FNSF) could play an important role in the development of fusion energy by providing the nuclear environment needed to develop fusion materials and components. The spherical tokamak (ST) is a leading candidate for an FNSF due to its potentially high neutron wall loading and modular configuration. A key consideration for the choice of FNSF configuration is the range of achievable missions as a function of device size. Possible missions include: providing high neutron wall loading (1-2MW/m$^2$) and fluence (3-6MWy/m$^2$), demonstrating tritium self-sufficiency (tritium breeding ratio TBR $\geq$ 1), and demonstrating electrical self-sufficiency. All of these missions must also be compatible with a viable divertor, first-wall, and blanket solution. During the past two years, U.S. studies have for the first time developed ST-FNSF configurations simultaneously incorporating: (1) a blanket system capable of TBR $\approx$ 1, (2) a poloidal field (PF) coil set supporting high $\beta$ and $\kappa$ for a range of $l_i$ and $\beta_N$ values consistent with NSTX/NSTX-U previous/planned operation, (3) a long-legged / Super-X divertor analogous to the planned MAST-U divertor which substantially reduces projected peak divertor heat-flux and has all outboard PF coils outside the vacuum chamber and as superconducting to reduce power consumption, and (4) a vertical maintenance scheme in which blanket structures and the centerstack (CS) can be removed independently. Progress in these ST-FNSF mission vs. configuration studies including dependence on plasma major radius $R_0$ for a range $R_0$ = 1m to 1.7m are described. In particular, it is found the threshold major radius for TBR ~ 1 is $R_0 \geq$ 1.7m, and a smaller $R_0$=1m device has TBR ~ 0.9 which is below unity but substantially reduces T consumption relative to not breeding. TRANSP/NUBEAM calculations of negative neutral beam heating and current drive in support of full non-inductive operation are also discussed.

## 1. Introduction

There are several pathways from ITER to a commercial power plant. One option is a fusion demonstration power plant (DEMO) [1] with an engineering/electricity gain $Q_{eng}$ ~ 3-5 and other parameters approaching those of a first of a kind power plant. Another option is a "Pilot Plant" which is a potentially attractive next-step towards fusion commercialization by demonstrating generation of a small amount of net electricity $Q_{eng} \geq 1$ as quickly as possible and in as small a facility as possible in a configuration directly scalable to a power plant [2]. However, there are significant challenges to achieving net electricity and tritium fuel production – in particular the blanket technology used for thermal power conversion and tritium breeding. Such challenges have motivated consideration of a Fusion Nuclear Science Facility (FNSF) / Component Test Facility (CTF) [2-8] to provide fusion-relevant neutron wall loading (1MW/m$^2$) and neutron fluence 6MW-yr/m$^2$ to develop and test fusion blankets. This paper assesses the Spherical Tokamak (ST) approach for an FNSF/CTF and in particular the achievable missions as a function of device size. The expectation is that smaller devices may be less costly to build and operate from an electricity consumption standpoint, but could not achieve tritium self-sufficiency.

This paper describes an assessment of two ST device sizes with major radii $R_0$=1.7m and $R_0$=1m to begin to address several key questions:

1. How large must an ST device be to achieve tritium breeding ratio TBR ≥ 1?
2. How much externally supplied tritium would be needed for a smaller ST that cannot achieve TBR ≥ 1?
3. What are the device and component lifetimes?

## 2. Physics Design

A key constraint on the design of an ST-based FNSF is the achievable shaping – namely the plasma boundary elongation κ and triangularity δ as a function of plasma aspect ratio A ≡ $R_0$/a, current profile peaking (internal inductance $l_i$), normalized pressure $\beta_T \equiv 2\mu_0\langle p\rangle/B_{T0}^2$, and normalized beta $\beta_N \equiv \beta_T$ a•$B_{T0}$ / $I_P$ [%mT/MA]. Figure 1 shows the elongation κ vs. internal inductance $l_i$ achieved on NSTX for a range of aspect ratios, and achievement of 5-10% higher κ will be assessed on NSTX-U utilizing improved vertical control. The ST-FNSF design assumption used in this paper is consistent with NSTX/NSTX-U as shown by the dashed line in Figure 1 and follows $\kappa_{x\text{-point}} = \kappa_{max\text{-}ST}(l_i) \equiv 3.4 - l_i$.

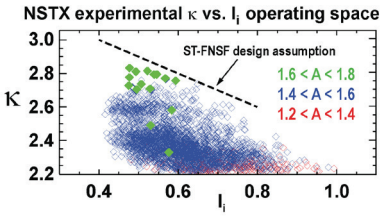


***FIG. 1** - NSTX elongation vs. internal inductance and ST-FNSF design assumption*

Figure 2 shows the coil, vessel, divertor, and blanket configuration for a $R_0$ = 1.7m ST-FNSF consistent with achieving equilibria with aspect ratio A=1.7-1.8, $\kappa_x = \kappa_{max\text{-}ST}(l_i)$, and triangularity $\delta_x$ = 0.54-0.6. This configuration and PF coil set has several important features including:

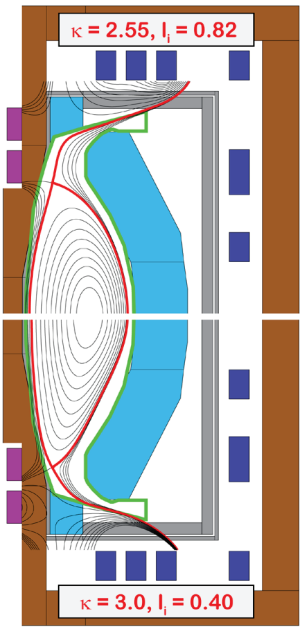


***FIG. 2** – $R_0$ = 1.7m ST-FNSF: TF coils (brown), divertor / outboard PF coils (purple / dark blue), vessel and shielding (gray), breeding blankets (light blue), limiter outline (green), and plasma poloidal flux contours (black and red). Upper / lower plots are $l_i$ = 0.82 / 0.40 and κ = 2.55 / 3.0.*

1. No equilibrium PF coils inside the vacuum vessel
2. Increased strike-point radius $R_{sp} \approx 1.5\text{-}1.6\times R_0$ which reduces |B| and $q_{||}$ at the divertor strike-point and partially shields the strike-point PFCs with the blankets. This configuration is similar to the Super-X divertor [9] to be tested on MAST-U in the near-term [10].
3. Secondary X-points outside the primary X-points (i.e. snowflake-like [11] features) which help to re-direct the divertor leg radially outward and increase field-line-lengths in the scrape-off-layer (SOL) which lowers detachment thresholds.
4. Support of a wide range of internal inductance $l_i$ = 0.4-0.8 (as shown in Figure 2) where the elongation and squareness change with $l_i$ variation while maintaining a fixed $R_{sp}$ and controllable total B-field angle of incidence $\theta_B$ of ≥ 1°.
5. Divertor PF coils in the ends of the central TF coil to support the strongly shaped equilibrium and high triangularity for stable high-β plasma operation.
6. Divertor strike-points at large major radius leaving space for breeding in the center-stack (CS) ends which is important for maximizing TBR in the ST configuration.

Importantly, as shown in Figure 3, the projected peak divertor heat flux $q_{\perp\text{-max}}$ for the proposed Super-X/snowflake divertor can be reduced by up to a factor of 3 relative to a conventional divertor to $\leq$ 10MW/m$^2$ even for nominally attached conditions for surface-average neutron wall loading $\langle W_n \rangle$ = 1MW/m$^2$. The case shown is for a $R_0$ = 1.7m configuration with $P_{fusion}$ = 160MW and $P_{NNBI}$ = 80MW for $Q_{DT}$ = 2. These heat-flux calculations assume the integral heat-flux width $\lambda_{q\text{-int}} > 2$mm, or equivalently that for a parallel heat flux width $\lambda_q$ = 0.8mm estimated from multi-machine scalings [12], the private-flux-region heat-flux diffusion scale length S is $\geq$ 0.8mm consistent with S $\approx \lambda_q$ as may be the case for more closed divertors and for small $\lambda_q$ < 1mm. Partial detachment is expected to further reduce the peak heat flux by another factor of 2-5 (possibly a factor of 10) [13,14] which could allow even higher $\langle W_n \rangle$ up to 2MW/m$^2$ with acceptable divertor heat flux and/or support smaller S and $\lambda_q$ if necessary. This coil set can also maintain fixed $R_{sp}$ and $\theta_B$ for the expected operating range $\beta_N$ = 0 – 6. For this $l_i$ and $\beta_N$ range, the outboard squareness varies from $\zeta_{out}$ = -0.15 to 0.1 and the CS and blanket shapes are consistent with this range.

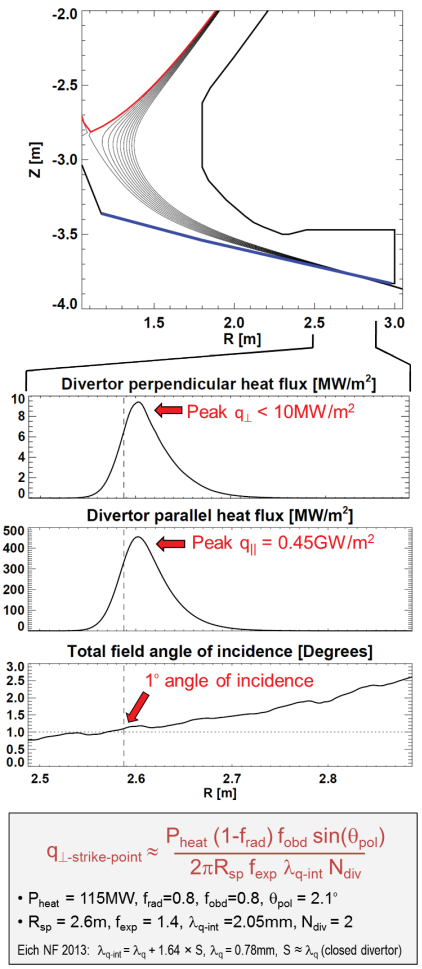


*FIG. 3 – Heat flux profiles, field-line angle of incidence, and assumed divertor parameters for estimating ST-FNSF peak heat flux.*

A very important consideration for ST-FNSF is the choice of heating and current drive source. Due to the typically over-dense plasma conditions of the ST, most RF schemes (ECCD, LHCD) are challenging or inapplicable, so neutral beam injection (NBI) heating is one of the few potential options. Indeed, nearly all the present high-performance ST physics basis has been developed using NBI heating. Further, momentum injection will be very important for providing rotation shear to suppress ion turbulence to achieve high ion temperatures for fusion applications, and tangential NBI can provide such rotation and rotation shear. Figure 4 shows how negative neutral beam injection (NNBI) current drive efficiency (in kA/MW) scales with injection energy and tangency radius of injection. As shown in the figure, the current drive efficiency increases rapidly with injection energy from 0.1-0.35MeV, then increases more slowly up to 0.5MeV, and above 0.5MeV increases little or begins to decrease slightly at large $R_{tan}$ due to shine through. The maximum CD efficiency is achieved for $R_{tan}$ = 2.3-2.4m for the $R_0$=1.7m ST device. Thus, the optimal injection energy is apparently 0.5MeV, and the optimal radius range is approximately $R_{tan}$ = 1.7-2.4m to control J(r) and $q(0)/q_{min}$ while avoiding excessive shine-through at larger $R_{tan}$.

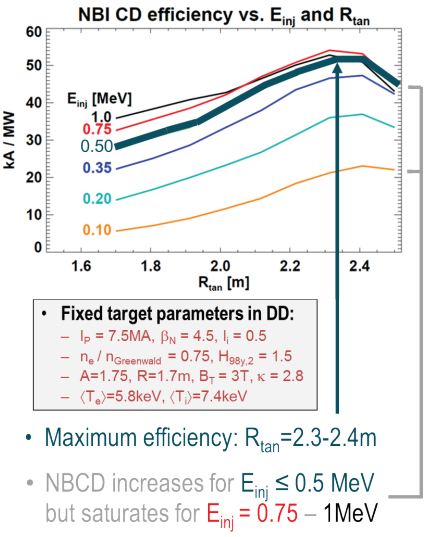


*FIG. 4 – NNBI current drive efficiency vs. injection energy $E_{inj}$ and injection tangency radius $R_{tan}$ in a fixed DD target plasma.*

Figure 5 shows free-boundary TRANSP [15] and NUBEAM [16] calculations of the profiles of temperature, current drive, density, and safety factor assuming neoclassical ion thermal diffusivity, scaled NSTX electron temperature and density profiles, and 80MW of 0.5MeV NNBI injected with a mix of near-axis and larger $R_{tan}$ injection to provide both on-axis and off-axis current drive to supplement the bootstrap current and maintain $q_{min} > 2$. Additional variations of injection radius, density, and confinement can be used to modify the minimum q and q-shear in the core region. As is evident from the figure, such scenarios with neoclassical ion confinement lead to hot-ion modes with $T_i > T_e$.

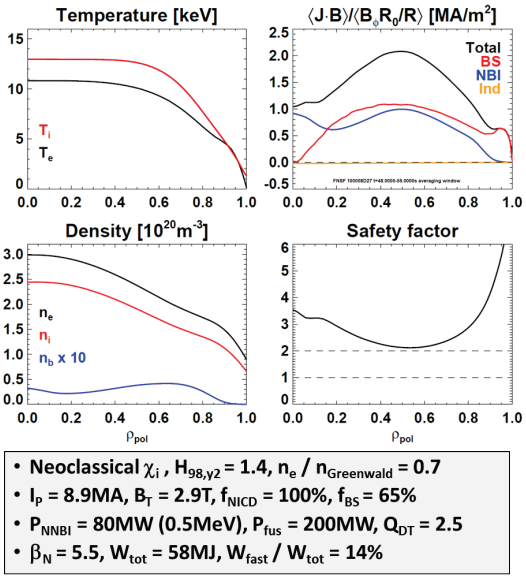


***FIG. 5** – TRANSP/NUBEAM calculations of a 100% non-inductively-driven 50-50DT plasma with $P_{fusion}$ = 200MW, $Q_{DT}$ = 2.5*

## 3. Device configuration

With the above definition of the plasma equilibrium, PF and TF coil location and size, vacuum vessel layout, blanket and divertor geometry, and NBI tangency radii, 3D CAD models of the ST-FNSF have been generated as shown in Figure 6 for the $R_0$=1.7m device. The lower graphic in Figure 6 shows an example test-cell layout (extrapolated from the ITER test cell configuration) showing NNBI injectors surrounding the device assuming a design similar to the JT-60SA NNBI injecting up to 20MW per port with 4 ports for 80MW total. As seen in the figure, the top superstructure, horizontal TF legs, and top PF coils and lid, can all be removed vertically. The TF center-stack and/or full blanket assembly or individual blanket modules can be removed independently. Divertor cooling and pumping and tritium breeding manifolds exit the device diagonally from the bottom and side of the device. Large copper leads for the TF coils and the associated power supplies are located underneath the machine in a lower test-cell chamber.

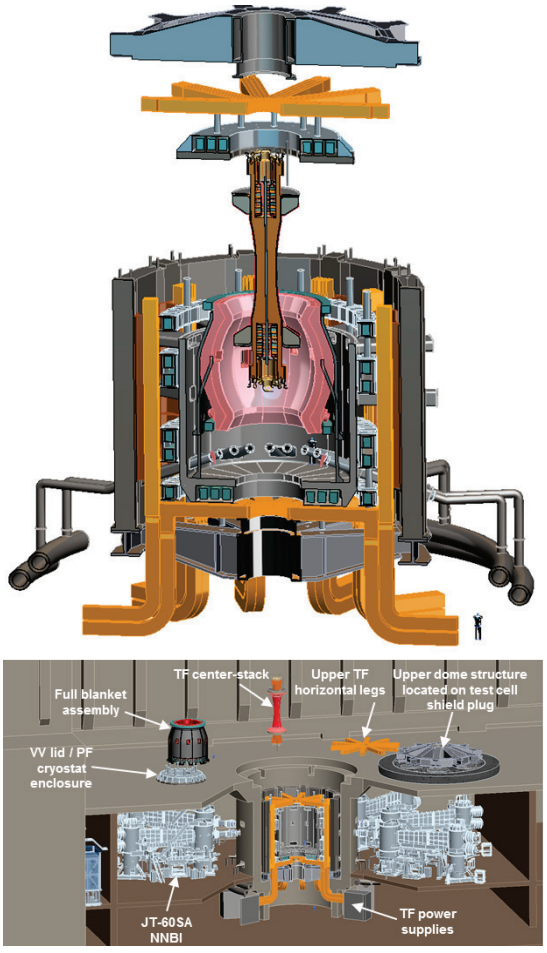


***FIG. 6** – (Top) Cross-section of $R_0$ = 1.7m ST-FNSF showing vertical maintenance strategy, (bottom) example layout of test-cell and components during maintenance.*

## 4. Neutron shielding and tritium breeding

Using the device configuration from Section 3, the shielding effectiveness and tritium breeding potential have been analyzed with sophisticated 3-D neutronics codes. In particular, the 3D CAD models have been coupled with MCNP using the University of Wisconsin DAGMC code [17] to accurately represent the entire torus. No approximations have been utilized in this analysis, and many configuration details are retained including:

1. 2 cm wide assembly gaps between toroidal sectors
2. Internals of two outboard (OB) dual-coolant lead-lithium (DCLL) blanket segments modeled in great detail, including the first-wall (FW), side, top/bottom, and back walls, cooling channels, and SiC flow-channel-inserts (FCI)
3. 2 cm thick W vertical stabilizing shells between OB blanket segments
4. Ferritic Steel (FS) port walls for test blanket / materials test modules (TBM / MTM) and NNBI

| Major Radius [m] | Minor radius [m] | Fusion Power [MW] | Average Neutron wall loading [MW/m$^2$] | # TF coils | # TBM ports | # MTM ports | # NBI ports |
|---|---|---|---|---|---|---|---|
| 1.68 | 0.95 | 162 | 1 | 12 | 4 | 1 | 4 |
| 1.00 | 0.57 | 62 | 1 | 10 | 4 | 1 | 3 |

***Table 1** – Parameters for $R_0$ = 1.7m and 1m ST-FNSF devices for shielding and TBR analysis.*

Two ST device sizes have been analyzed for shielding and TBR as shown in Table 1. For both sizes the assumed plant lifetime is ~20 years with an availability ranging from 10-50% with an average value of 30% equivalent to 6 full power years (FPY) of operation. Figure 7 shows neutron dose calculations at the corners of the PF coil regions in both the TF centerstack and also behind the divertor exhaust region. Assuming MgO insulation of Cu conductors for both the divertor PF coils in the TF in the centerstack and also the most inboard of the top and bottom divertor region PF coils, the neutron dose is well below (by at least 1 order of magnitude) the present best estimate of the allowable limit of $10^{11}$ Gy [18]. Thus, for the PF coils in the ends of the TF centerstack, the Cu of the TF bundle not only provides the conducting path for the TF coil current but also provides shielding for the inner-most divertor PF coils. This factor of 15 shielding margin is also adequate to shield the divertor PF coils in the smaller $R_0$ = 1m ST. The peak outboard dpa of 15.5 dpa / FPY implies 93 dpa total damage to the outboard first-wall for 6FPY of operation. This total dpa level is 9 times the current limit of 10 dpa for ferritic steel and calls for the development of more radiation resistant ferritic steel structures that can handle 100 dpa or more. The Test Blanket Modules (TBMs) and Materials Test Module (MTM) at the outboard midplane are subject to a fusion-

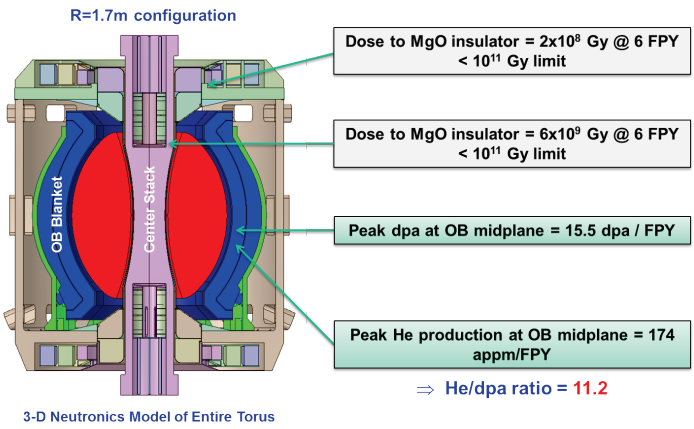


***FIG. 7** – Calculated peak neutron dose calculations at the divertor PF coils and peak dpa and He production at the outboard midplane blanket regions.*

relevant nuclear environment and will develop and test materials and components for fusion power production applications [19].

The calculated TBR for different components of the $R_0$ = 1.7m device is shown in Figure 8. As seen in the figure, the inner-most radial segment of the outboard blanket provides a TBR of 0.81, while the outer-most segment provides 0.15 for a total outboard blanket TBR of 0.96. Thus, to achieve TBR > 1 even with no penetrations or ports, additional breeding regions are needed. A key advantage of the long-legged Super-X/snowflake divertor is that the divertor strike-point region can be moved to larger major radius away from the relatively high neutron flux regions at the top and bottom ends of the centerstack. By breeding in these top/bottom end regions, the total TBR can be increased by an additional 0.07 for a total of 1.03.

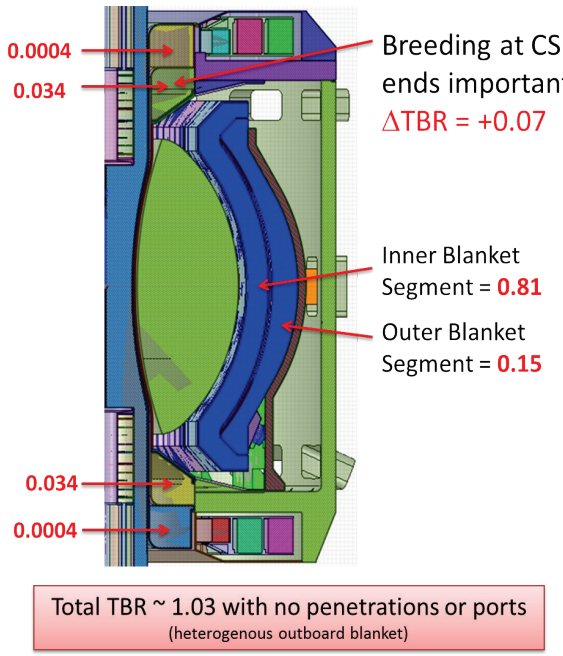


***FIG. 8** – TBR vs. component assuming no penetration or ports.*

Figure 9 shows the impact of including a range of midplane ports including 4 TBMs and 1 MTM with blanket front-face areas of 0.9m$^2$ each, and penetrations for the negative neutral beams with aperture areas of 0.4m$^2$ perpendicular to the beam-line. As shown in the figure, the TBMs provide breeding nearly as efficiently as the DCLL base blanket with an overall TBR reduction of only 1% (0.25% per TBM). In contrast, the MTM does not provide breeding which leads to a TBR reduction of 2% per port. Lastly, each of the 4 NNBI ports is sized to support 20MW of NBI power with a perpendicular aperture area of 0.4m$^2$ for an average port power density of 50MW/m$^2$ [20]. The total TBR reduction from all 4 NNBI ports is 3%, i.e. an average of 0.75% per NNBI. Including all 4 TBMs, 1 MTM, and 4 NNBI ports results in an overall TBR of 0.97.

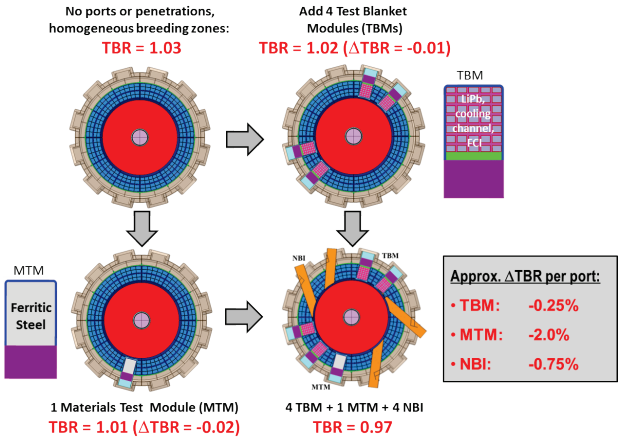


***FIG. 9** – Calculated TBR with modules and NBI penetrations included.*

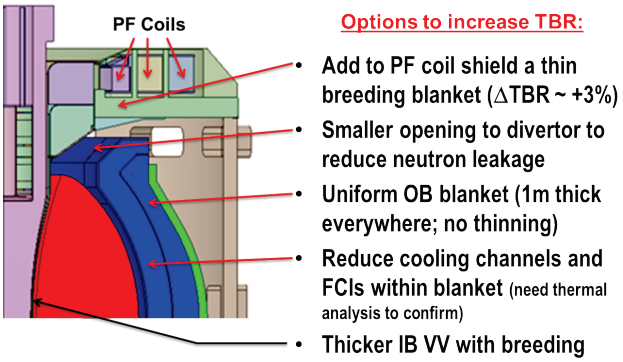


***FIG. 10** – Options for increasing TBR in the $R_0$ = 1.7m ST-FNSF.*

It is highly desirable to demonstrate tritium self-sufficiency in an FNSF device, and the calculated TBR for the $R_0$ = 1.7m ST-FNSF of 0.97 is very close to unity. Several ideas/options have been identified to further increase TBR to values above 1, and these ideas are shown in Figure 10. It is expected that some combination of these options will enable achievement of TBR ≥ 1 at the $R_0$ = 1.7m size. In contrast, the TBR for the $R_0$ = 1m configuration is found to be 0.88 which is far enough below 1 that even if the options to increase TBR shown in Figure 10 are exploited, the TBR will very likely still be below 1. Despite this (expected) inability to achieve TBR ≥ 1 in the relatively small $R_0$ = 1m device, TBR of 0.88 is still very substantial and would reduce the external supply of T by over a factor of 8 relative to not breeding any tritium.

Figure 11 shows the spatial distribution of the T production in the blanket and TBMs. Note that despite the significant area opened by the NBI penetrations, the very tangential injection allows streaming neutrons to be captured at the back of the blanket, thereby offsetting the reduction in TBR relative to what would be expected based on blanket front-face-aperture area scalings alone.

For the $R_0$=1m device it will be necessary to purchase ~0.4-0.55kg of T/FPY from outside sources at a cost of $30-100k/g of T implying a total cost of $12-55M/FPY. Since the expected average duty factor is 0.3, the estimated annual average cost for T is $4-17M per year which is likely an acceptable operating cost for a major nuclear device and associated program. However, there is uncertainty in relying on external sources to supply T fuel (~3 kg over 6FPY) for such a program. Finally, Figure 12 shows a side-by-side and to-scale summary comparison of the $R_0$=1.7m and 1m ST-FNSF configurations showing expected TBR values and TBM, MTM, and NBI ports layouts.

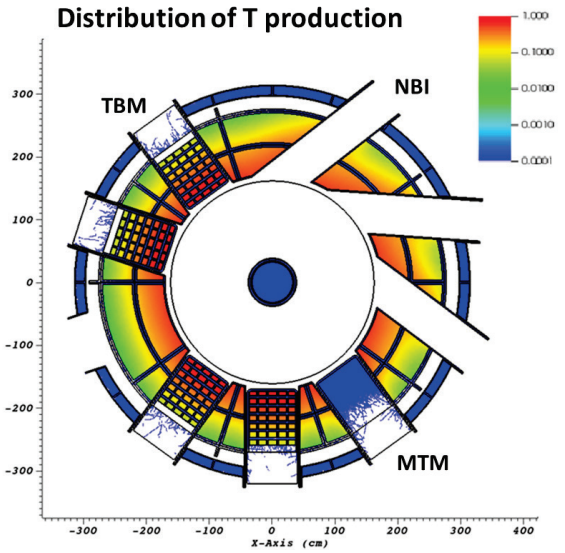


*FIG. 11 – Normalized tritium production distribution at the midplane of the $R_0$ = 1m ST-FNSF configuration.*

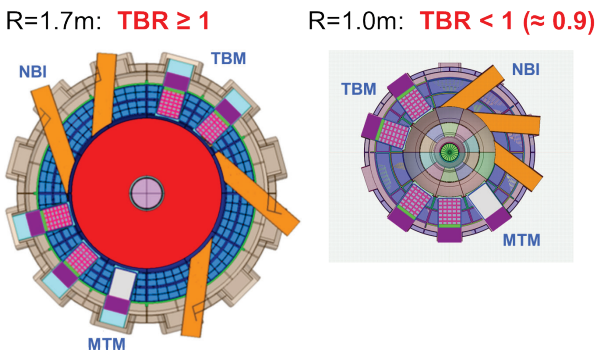


*FIG. 12 – Side-by-side comparison of mid-plane sections of $R_0$=1.7m and 1m ST-FNSF configuration showing TBR and TBM, MTM, and NBI ports.*

## 5. Summary

Substantial progress has been made in the last two years to advance the design concepts for an ST-based FNSF. Ex-vessel PF coil sets have been identified to support a range of equilibria and a Super-X/snowflake divertor to mitigate divertor heat flux to acceptable levels. Using TRANSP/NUBEAM analysis, NNBI with an injection energy of 0.5MeV appears optimal for heating and current drive for the $R_0$=1.7m size. An attractive vertical maintenance approach and plausible test-cell layout compatible with NNBI has been identified. Shielding of the

inboard PF coils appears adequate assuming MgO insulation, and the larger outboard PF coils (behind outboard blankets) can be superconducting. The full 3D TBR has been calculated to quantify the TBR reduction from TBMs, MTMs, and NBI ports. The threshold major radius for TBR ~ 1 is $R_0 \geq 1.7$m. A smaller R=1m device could provide TBR = 0.88 which is below unity, but substantially reduces the T consumption relative to not breeding. The external supply of T for the smaller device would be ~0.4-0.55kg of T/FPY or $12-55M/FPY. However, this $R_0$=1m device would have lower electricity consumption and capital cost. Future work will assess such size/cost trade-offs in more detail.

## 6. References


[1] F. Najmabadi, et al., The STARLITE project: the mission of the fusion demo, 16th IEEE Symp. on Fusion Engineering (Champaign, IL, 1995) http://www-ferp.ucsd.edu/NAJMABADI/PAPER/95-IEEE.pdf

[2] J. Menard, et al., Nuclear Fusion **51** (2011) 103014

[3] M. Peng, et al., Plasma Physics and Controlled Fusion **47** (2005) B263–B283

[4] M. Peng, et al., Fusion Science and Technology **56** (2009) 957

[5] G. Voss, et al., Fusion Engineering and Design **83** (2008) 1648–1653

[6] M. Kotschenreuther, et al., Fusion Engineering and Design **84** (2009) 83–88

[7] B. Kuteev, et al., Nuclear Fusion **51** (2011) 073013

[8] V. Chan, et al., Fusion Science and Technology **57** (2010) 66

[9] P.M. Valanju et al., Physics of Plasmas **16**, (2009) 056110

[10] G. Fishpool, et al., Journal of Nuclear Materials **438** (2013) S356–S359

[11] D. Ryutov, et al., Plasma Phys. Control. Fusion **52** (2010) 105001

[12] T. Eich, et al., Nuclear Fusion **53** (2013) 093031

[13] J. Canik, et al., 2013 IEEE Symposium on Fusion Engineering (DOI: 10.1109/SOFE.2013.6635482)

[14] E. Meier, et al., "Modeling divertor concepts for spherical tokamaks NSTX-U and ST-FNSF", paper TH/P6-50 this conference.

[15] R. J. Goldston, D.C. McCune, and H.H. Towner, J. Comput. Phys. **43** (1981) 61

[16] A. Pankin, et al., Computer Physics Communications **159** (2004) 157–184

[17] "DAGMC Users Guide," University of Wisconsin-Madison Fusion Technology Institute (2008); https://trac.cae.wisc.edu/trac/svalinn/wiki/DAGMCUsersGuide.

[18] K. Fan, et al., R&D of a Septum Magnet Using MIC coil, Proceedings of the 5th Annual Meeting of Particle Accelerator Society of Japan and the 33rd Linear Accelerator Meeting in Japan (August 6-8, 2008, Higashihiroshima, Japan)

[19] L. El-Guebaly, L. Mynsberge, J. Menard, T. Brown, S. Malang, and L. Waganer, "Nuclear Aspects and Blanket Testing/Development Strategy for ST-FNSF," IEEE Transactions on Plasma Science, 42, No. 5, 1457-1463 (May 2014).

[20] K. Tobita, et al., Nucl. Fusion **47** (2007) 892–899